



Article

Ectopic Expression of *Neurod1* Is Sufficient for Functional Recovery following a Sensory–Motor Cortical Stroke

Jessica M. Livingston ^{1,2}, Tina T. Lee ¹, Tom Enbar ^{1,2,3}, Emerson Daniele ^{1,3} , Clara M. Phillips ^{1,2}, Alexandra Krassikova ¹ , K. W. Annie Bang ⁴ , Ines Kortebi ^{1,3}, Brennan W. Donville ^{1,2}, Omadyor S. Ibragimov ¹, Nadia Sachewsky ^{1,2}, Daniela Lozano Casasbuenas ¹ , Arman Olfat ¹ and Cindi M. Morshead ^{1,2,3,5,*}

¹ Department of Surgery, Division of Anatomy, 1 King's College Circle, University of Toronto, Toronto, ON M5S 1A8, Canada; jmlivingston@hollandcollege.com (J.M.L.); emerson.daniele@mail.utoronto.ca (E.D.); ines.kortebi@mail.utoronto.ca (I.K.)

² Donnelly Centre for Cellular and Biomolecular Research, University of Toronto, 160 College Street, Toronto, ON M5S 3E1, Canada

³ Institute of Medical Science, 1 King's College Circle, University of Toronto, Toronto, ON M5S1A8, Canada

⁴ Lunenfeld-Tanenbaum Research Institute, 600 University Ave., Toronto, ON M5G 1X7, Canada; bang@lunenfeld.ca

⁵ Institute of Biomedical Engineering, 1 King's College Circle, University of Toronto, Toronto, ON M5S 1A8, Canada

* Correspondence: cindi.morshead@utoronto.ca; Tel.: +1-416-946-5575

Abstract: Stroke is the leading cause of adult disability worldwide. The majority of stroke survivors are left with devastating functional impairments for which few treatment options exist. Recently, a number of studies have used ectopic expression of transcription factors that direct neuronal cell fate with the intention of converting astrocytes to neurons in various models of brain injury and disease. While there have been reports that question whether astrocyte-to-neuron conversion occurs in vivo, here, we have asked if ectopic expression of the transcription factor *Neurod1* is sufficient to promote improved functional outcomes when delivered in the subacute phase following endothelin-1-induced sensory–motor cortex stroke. We used an adeno-associated virus to deliver *Neurod1* from the short GFAP promoter and demonstrated improved functional outcomes as early as 28 days post-stroke and persisting to at least 63 days post-stroke. Using *Cre*-based cell fate tracking, we showed that functional recovery correlated with the expression of neuronal markers in transduced cells by 28 days post-stroke. By 63 days post-stroke, the reporter-expressing cells comprised ~20% of all the neurons in the perilesional cortex and expressed markers of cortical neuron subtypes. Overall, our findings indicate that ectopic expression of *Neurod1* in the stroke-injured brain is sufficient to enhance neural repair.

Keywords: direct lineage conversion; *Neurod1*; brain repair; stroke; functional recovery; ectopic transcription factor expression; adeno-associated virus; astrocyte-to-neuron conversion; neuroregeneration; gait analysis



Citation: Livingston, J.M.; Lee, T.T.; Enbar, T.; Daniele, E.; Phillips, C.M.; Krassikova, A.; Bang, K.W.A.; Kortebi, I.; Donville, B.W.; Ibragimov, O.S.; et al. Ectopic Expression of *Neurod1* Is Sufficient for Functional Recovery following a Sensory–Motor Cortical Stroke. *Biomedicines* **2024**, *12*, 663.

<https://doi.org/10.3390/biomedicines12030663>

biomedicines12030663

Academic Editor: Xuanyu Chen

Received: 31 January 2024

Revised: 5 March 2024

Accepted: 11 March 2024

Published: 15 March 2024



Copyright: © 2024 by the authors. Licensee MDPI, Basel, Switzerland. This article is an open access article distributed under the terms and conditions of the Creative Commons Attribution (CC BY) license (<https://creativecommons.org/licenses/by/4.0/>).

1. Introduction

Stroke is a leading cause of death and disability worldwide, and many survivors experience long-lasting impairments [1]. Approximately 850,000 individuals in North America suffer from strokes annually [2]. Survivors often experience motor impairments, particularly affecting sensory-motor function in the upper limbs [2]. This can lead to chronic disability that significantly diminishes quality of life and increases the risk of post-stroke depression [3]. With an aging population and increasing projected incidence of stroke [4], there is an urgent need for alternative options to improve post-stroke impairments.

Numerous approaches to treat stroke have been explored, including activation of endogenous neural stem cells [5–7] and cell transplantation [8,9]. Since the discovery that ectopic transcription factor (TF) expression can drive cell fate [10], attention has been

focused on developing interventions to replace lost cells in models of injury or disease. Many publications have since identified effective methods to convert somatic cells to other cell types [11,12], including neuronal cells, both in vitro and in vivo [13–22]. In the context of the central nervous system (CNS), a number of groups have examined the ectopic expression of TFs in the CNS and demonstrated that proneural TFs such as Ngn2 [23] and Ascl1 [20,24] and the neuronal differentiation TF Neurod1 [25,26] can convert glial cells to neurons [27]. Further, studies have shown that induced neurons from the ectopic expression of TFs have regionally appropriate [14,28,29] and functional neuronal subtype identities [15,30–33]. Some recent studies in the field have brought into question the efficacy of in vivo conversion [34,35], and this has served to highlight the importance of addressing potential caveats to further advance the field [19,36,37]. Wang et al. [34] reported off-target neuronal expression of adeno-associated virus (AAV)-based delivery strategies driving TF expression from the short human GFAP promoter (shGFAP). While the mechanism is not entirely understood, the implication is that transduced endogenous neurons could mistakenly be interpreted as astrocyte-to-neuron reprogramming [34,35]. Nevertheless, the report by Wang et al. [34] does not negate the capacity of glia to be converted to neurons [27,38,39].

Of particular interest in developing therapeutics to promote neural repair, a number of groups have validated the feasibility of ectopic TF expression in preclinical models of injury and disease, including Alzheimer's disease [40], Parkinson's disease [41], and stroke [26,42]. These studies have focused on cellular outcomes, and a considerable gap exists in understanding the resulting functional outcomes of the AAV-mediated ectopic expression of neural TFs. Acknowledging that endogenous neurons may be targeted to overexpress TFs delivered by AAVs underscores the possibility that ectopic expression of TFs in neurons may underlie any improved outcomes, making this approach promising to treat neurological disease. Hence, it is important to study the functional outcomes of forced TF expression-based therapy. To this end, in a study of Parkinson's disease, the ectopic expression of a cocktail of TFs that promote dopaminergic cell fate in astrocytes improved some aspects of motor function [41]. Further, improved functional outcomes were recently reported using the TF *Neurod1* in a rodent ischemia model [42]. While these studies highlight the promising potential of gene therapy for neurorepair and functional recovery there is caution when advancing the translation of preclinical studies. For example, translating preclinical stroke research has not proven successful, and a number of recommendations and guidelines have been put forth by the Stroke Therapy Academic Industry Roundtable (STAIR) to overcome this challenge, including the rigorous testing and replication of potential therapeutics in more than one preclinical model [43].

Herein, we aimed to understand the longer-term functional outcomes of ectopic TF expression. We used AAV-mediated delivery of *Neurod1* to GFAP-expressing cells in a well-established preclinical model of sensory-motor ischemic stroke. The endothelin-1 model [44,45] has the advantage of generating highly reproducible lesions and controlled and persistent deficits in upper limb function, making it useful for studying post-stroke recovery strategies. Different from the published stroke studies of Chen and colleagues [42], we chose a different AAV serotype to deliver *Neurod1* based on reports suggesting enhanced astrocyte targeting with AAV5 [46]. Further, the previous stroke study used the ubiquitous CAG promoter to drive TF expression. Herein, *Neurod1* expression was under the control of the short GFAP (gfaAVC(1)D) promoter to further target astrocyte-driven expression. We performed our experiments in a conditional reporter mouse that enabled us to track transduced cells and performed functional assays up to 9 weeks post-stroke. We found that ectopic expression of *Neurod1* delivered in a sub-acute phase post-cortical stroke led to persistent improved motor outcomes. Virally transduced cells expressed cortical layer-appropriate neuronal markers. These findings provide further support that ectopic expression of *Neurod1* is a viable approach to improve stroke recovery.

2. Materials and Methods

2.1. Mice

Adult (8–12 week old) male and female R26R-YFP (Jackson Labs, Bar Harbor, ME, USA: B6.129X1-*Gt(ROSA)26Sortm1(EYFP)Cos/J*) and R26R-tdTomato (Jackson Labs: *Gt(ROSA)26Sortm9(CAG-tdTomato)Hze*) mice were used in this study [47]. Mice were group-housed in a barrier facility with a 12 h light/12 h dark cycle with ad libitum access to food and water. Experiments were conducted according to protocols approved by the Institutional Animal Care Committee and performed in accordance with guidelines published by the Canadian Council for Animal Care.

2.2. Endothelin-1 Stroke

The vasoconstricting peptide endothelin-1 (ET-1; Calbiochem, San Diego, CA, USA) was used to induce focal stroke to the sensory–motor cortex as previously described [9,48]. Mice were anesthetized using isoflurane and mounted onto a stereotaxic apparatus. The scalp was incised, and a small hole was drilled into the skull at the injection location. A total of 1 μ L of 400 picomolar ET-1 dissolved in sterile PBS was injected into the sensory–motor cortex at +0.6 AP, +2.20 ML, and –1.0 DV from bregma. A 26-gauge Hamilton syringe with a 45-degree beveled tip was used to inject ET-1 at a rate of 0.1 μ L/min. The needle was left in place for 10 min after completion of the ET-1 injection to prevent backflow, then slowly withdrawn. Body temperature was maintained at 37 °C using a heating pad, and animals recovered under a heat lamp. Ketoprofen (5.0 mg/kg; s.c.) was administered for post-surgery analgesia.

2.3. Adeno-Associated Virus (AAV) Injections

AAV5-GFAP(0.7)^{promoter(gfaABC(1)D)}::*Neurod1*-T2A-Cre-WPRE (AAV5::*Neurod1*; 5.0×10^{12} GC/mL) and AAV5-GFAP(0.7)^{promoter(gfaABC(1)D)}-Cre-WPRE (AAV5::*Cre*; 1.1×10^{13} GC/mL) were generated and packaged by Vector BioLabs (Malvern, PA, USA).

Mice were anesthetized with isoflurane and mounted onto a stereotaxic apparatus. A total of 1 μ L of AAV5::*Neurod1* or AAV5::*Cre* was injected into the ipsilesional cortex 7 days post-stroke or -sham injury, at a rate of 0.1 μ L/min at each the following coordinates: [+0.6 AP, +2.2 ML, –1.0 DV], [+1.6 AP, +2.2 ML –1.0 DV], and [–0.4 AP, +2.2 ML, –1.0 DV] mm from bregma, representing regions encompassing the anterior-to-posterior extent of the stroke-lesioned brain. The needle was left in place for 10 min after each AAV injection to prevent backflow and then slowly withdrawn. Body temperature was maintained at 37 °C using a heating pad, and animals recovered under a heat lamp. Ketoprofen (5.0 mg/kg; s.c.) was administered for post-surgery analgesia.

2.4. Tissue Processing, Immunohistochemistry, Imaging, and Quantification

Mice were anesthetized with tribromoethanol (Avertin; 250 mg/kg; i.p.) and perfused transcardially with saline, followed by 4% paraformaldehyde (PFA). Brains were removed, post-fixed for 4 h with 4% PFA, and then placed in 30% sucrose to cryopreserve. Brains were frozen, sectioned (20 μ m) using a cryostat, mounted onto Superfrost Plus slides, and stored at –20 °C.

For immunohistochemistry, slides were sectioned, blocked with 10% normal goat serum (NGS) and 0.3% Triton x-100 in PBS, and labeled with primary antibodies (for astrocytes, rabbit-anti-GFAP was used, 1:3000, DAKO, Santa Clara, CA, USA, 2016-04; or chicken-anti-GFAP, 1:1000, Aves, GFP-1020. For neurons, rabbit-anti-NeuN was used, 1:100, Millipore, Oakville, ON, Canada, ABN78. For layer-specific markers, the upper-layer marker rabbit-anti-CUX1 was used, 1:100, Abcam, Baltimore, MA, USA, AB54583; and the lower-layer marker rat-anti-CTIP2, 1:300, Abcam, AB18465. To detect evidence of activity, the early immediate gene protein mouse-anti-cFOS was used, 1:200, Santa Cruz, Dallas, TX, USA, Sc-166940. To determine the cell phenotype as oligodendrocyte, microglia, or migratory neuroblasts, Olig 2, 1:500, Millipore, Iba1, 1:500, Wako, Richmond, VA, USA were used) in PBS overnight at 4 °C, followed by incubation with secondary antibodies

(1:400, from Life Technologies (Carlsbad, CA, USA): goat-anti-rabbit 568; goat-anti-rabbit 647; goat-anti-chicken 488; goat-anti-mouse 488) and DAPI (1:10,000; Invitrogen, Waltham, MA, USA) in PBS for 1 h at room temperature. Slides were then cover-slipped using Dako fluorescent mounting media (ThermoFisher, Waltham, MA, USA).

Imaging was performed using Zen 2011 (v.1.0) software and a Zeiss confocal microscope (LSM880, v.14, Zeiss, Oberkochen, Germany). Linear contrast/brightness adjustments were performed using Zen 2011 software or Adobe Photoshop (v.20). Colocalization analysis was performed by z-stack analysis to confirm overlapping expression in confocal images in three images from three different coronal sections (located at +1.6, +0.6, and −1.0 AP from bregma) per animal viewed at 20× magnification. Identical linear adjustments of contrast and brightness were made to micrographs using the respective microscope software or Photoshop using the levels function, as follows: CUX1 (linear brightness adjustment, all channels), TBR1 (linear brightness adjustment, red channel), CTIP2 (linear brightness adjustment, red channel), and c-FOS (linear brightness adjustment, green channel).

2.5. Lesion Volume Analysis

Lesion volume was calculated from NeuN-stained sections and defined as areas devoid of NeuN+ stain. Image J (v.2, National Institute of Health, New York, NY, USA) was used to measure this area in 5 × 20 μm thick coronal sections (160 μm apart) spanning the anterior–posterior extent of the injury site. The software was calibrated using a scale bar, and the area measurement was obtained using the freehand selection tool. Area was then multiplied by the distance between sections to estimate the total infarct volume.

2.6. Astrocyte Sorting and ImageStream Analysis

Mice were anesthetized with isoflurane and cervically dislocated. The brain and meninges were removed, and coronal slices were obtained using a scalpel blade. The cortex was collected from slices that included the lesioned cortex, taking care to avoid the corpus callosum. The tissue was enzymatically and mechanically dissociated into a single-cell suspension using the magnetically activated cell-sorting (MACS) Neural Tissue Dissociation Kit (Miltenyi Biotec, Bergisch Gladbach, Germany, 130-093-231). Myelin was removed using the MACS Myelin Removal Beads (Miltenyi Biotec 130-096-733). Dissociated cells were resuspended in 500 μL of PBS (azide and serum/protein free) and stained with a fixable cell viability dye (FVD eFluor 780; eBioscience, San Diego, CA, USA, 65-0865-14) according to the manufacturer's instructions (1 μL FVD/mL cell suspension). Cells were washed with 10% FBS in PBS, then resuspended in 500 μL of MACS buffer (Ca⁺⁺ and Mg⁺⁺ free PBS with 2% FBS and 1 mM EDTA), stained with anti-GLAST-PE (1:50; Miltenyi Biotec 130-098-804), and sorted using the MACS anti-PE MicroBeads UltraPure Kit (Miltenyi Biotec 130-105-639) according to the manufacturer's instructions. Sorted cells were stained with Hoescht (1 μg/mL, BD Biosciences, San Diego, CA, USA, 33342) for 30 min at room temperature, then resuspended in MACS sorting buffer.

Cells were analyzed with an Amnis ImageStream Mark II imaging flow cytometer (AMNIS). Cells from the MACS sorted fractions and column flow-through were analyzed. Single-stained controls were collected for the compensation matrix to determine the level of spectral overlap (live nucleated cells were examined for PE-GLAST signal and YFP). The resulting compensated image files were analyzed using IDEAS analysis software (AMNIS, v.6.0). For the analysis, focused single cells were selected based on viability (excluding FVD e780 dye) and the presence of a nucleus (Hoescht-positive). The live nucleated cells were examined for PE-GLAST signal, and the specific and punctate GLAST-PE binding to cells was described using the Bright Detail Intensity feature in IDEAS software v.6.0). The antibody binding patterns were confirmed in composite cell images of bright field and PE fluorescence generated from ImageStream data.

2.7. Foot Fault Analysis

Mice were placed onto a metal grid (1 cm spacing) that was suspended 12 inches above a table surface. Animals were allowed to walk around the grid for 3 min and were recorded from below. The number of steps and paw slips made with each forelimb were analyzed, and the difference in foot faults was calculated as follows: $\%slippage = [(\#slips/\#steps_{\text{ispilesional}}) - (\#slips/\#steps_{\text{contralesional}})]$. The following inclusion criteria were applied: (i) demonstrated deficit following stroke (defined as ± 2 standard deviations from the mean of uninjured controls at PSD 4), (ii) >50 steps taken during the test. These criteria resulted in the exclusion of a total of 5 mice from the study.

2.8. Gait Analysis

Gait analysis was performed using the automated Noldus CatWalk XT system (Noldus, Wageningen, The Netherlands). Mice were allowed to traverse a glass walkway illuminated with a light, and a number of gait parameters were measured. Mice were pre-trained to cross the platform for 2–3 consecutive days prior to stroke. A minimum of 3 successful trials was required, wherein the speed during crossing did not vary more than 60%. Footprints were recorded using a high-speed video camera and analyzed using CatWalk XT software (v.10.6). Parameters were normalized to the performance of uninjured mice and compared between both stroke groups and *Cre*-injected shams. Parameters that were significantly different between groups at baseline were excluded from analysis.

2.9. Data Acquisition and Statistical Analysis

All experiments were conducted by an experimenter blind to injury and treatment conditions. Data were tested for normality using the D'Angostino and Pearson omnibus normality test or the Kolmogorov–Smirnov test. Unpaired one-tailed *t*-tests were used to compare two groups. One-factor analysis of variance (ANOVAs) followed by post hoc analysis (Tukey's or Dunnet's test) was used to compare 3 or more groups. Foot fault outcomes were analyzed using 2-way repeated measures ANOVA, followed by Bonferroni post hoc tests when appropriate. Lesion volume was analyzed using Mann–Whitney U test. Differences were considered significant at $p < 0.05$. Values are presented as mean \pm SEM.

3. Results

3.1. Transduced Cells Persist Long Term

We designed a strategy to deliver *Neurod1* to GFAP+ cells in the stroke-injured cortex. AAV5::*Neurod1* or AAV5::*Cre* control was injected into the injured cortex of *Cre*-conditional reporter mice (R26R-YFP or R26R-tdTomato) on post-stroke day 7 (PSD7) (Figure 1a,b), a time that reflects the subacute phase of injury. To first determine the profile of transduced cells using this delivery strategy, mice were sacrificed at day 5 post-AAV5::*Cre* injection (PSD12). As predicted, the vast majority of transduced (tdTom+) cells expressed GFAP (Figure 1c,d); a small percentage of cells co-expressed the neuronal marker NeuN. A rare tdTom+ cell co-localized with the microglia/macrophage marker Iba1. None of the tdTom+ cells were neuroblasts (DCX+) or oligodendrocytes (Oligo2+) at 5 days post-AAV delivery.

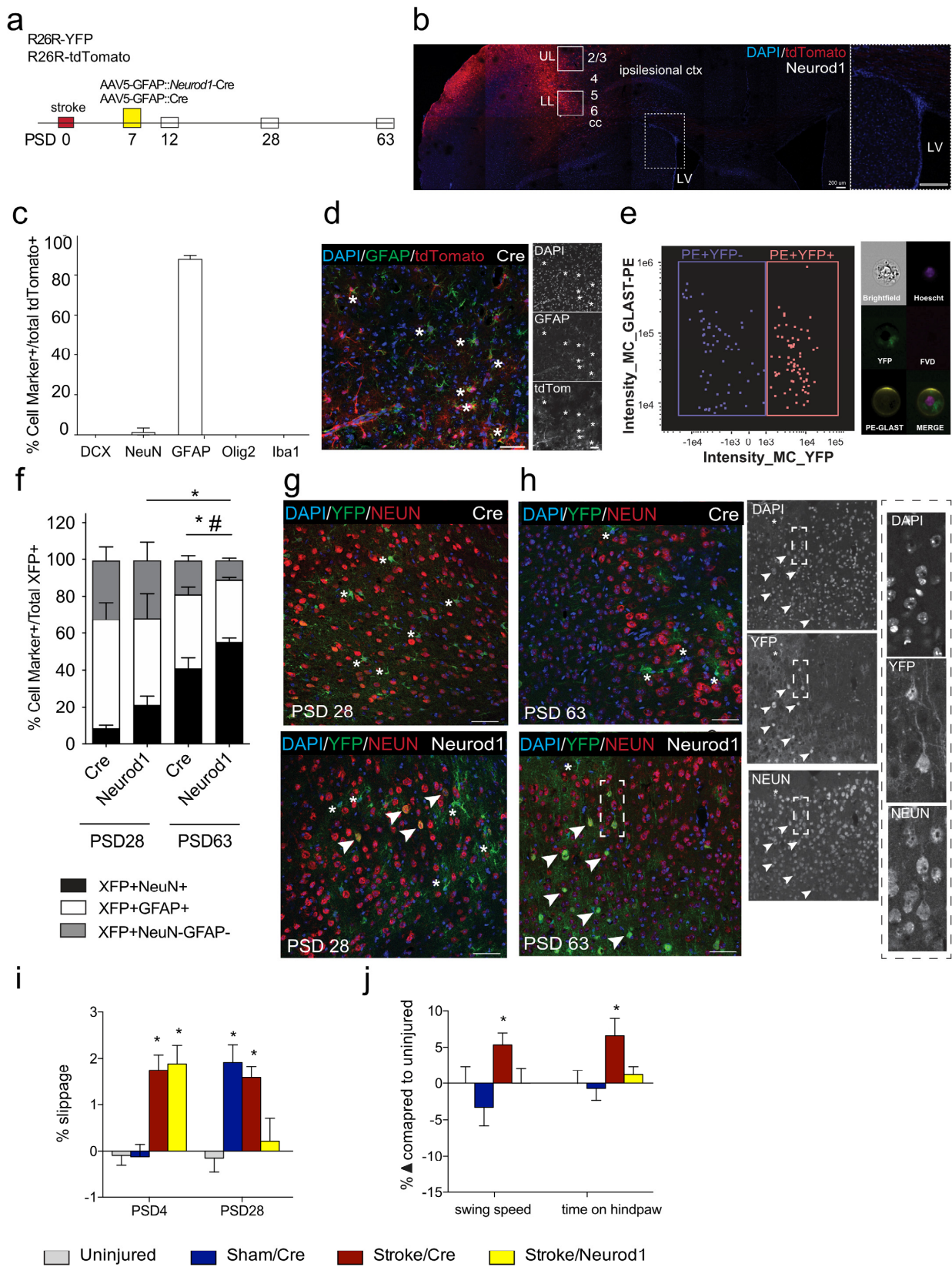


Figure 1. Astrocyte transduction following AAV5-based gene delivery. (a) Experimental design and timeline. (b) Example image of a stroke-injured cortex 5 days after viral transduction. Dashed box shows enlarged image of the neurogenic subependymal zone (SEZ). (c) Quantification of cell type marker expression in transduced cells at 5 days post-Cre; $n = 4$ /group. (d) Example image of transduced astrocytes

in a *Cre*-injected brain. Asterisks indicate examples of GFAP+tdTomato+ cells. Scale bar = 100 μm . (e) ImageStream plot of MACS sorted GLAST-PE+ astrocytes (40 \times magnification). Example image of a single (brightfield), live [fixable viability dye (FVD-)], nucleated (Hoechst+), GLAST-PE+YFP+ astrocyte. ($1\text{e}3 = 1 \times 10^3$, $1\text{e}4 = 1 \times 10^4$, $1\text{e}5 = 1 \times 10^5$, $1\text{e}6 = 1 \times 10^6$, $-1\text{e}3 = 1 \times 10^{-3}$, $-1\text{e}3 = 1 \times 10^{-3}$) (f) Quantification of the percentage of transduced cells that were NeuN+ (black bars), GFAP+ (gray bars), and neither (white bars). * $p < 0.05$, XFP+NeuN+ in *Cre* vs. *Neurod1*; # $p < 0.05$ XFP+NeuN-GFAP-comparison in *Cre* vs. *Neurod1*; $n = 3\text{--}9/\text{group}$. Data are expressed as mean \pm SEM. (g) Example images of *Cre*- and *Neurod1*-treated stroke-injured brains at PSD28 and (h) PSD63. Stars = transduced astrocytes; arrowheads = transduced astrocytes expressing NeuN. White dashed box shows enlarged image of transduced astrocytes expressing NeuN. Scale bars = 50 μm . (i) Percent slippage in the foot fault test revealed significant impairment in stroke-injured mice prior to reprogramming (PSD4) that was recovered by PSD28 in *Neurod1*-treated mice. A transient deficit was detected at PSD28 in *Cre*-injected sham control mice. $n = 6\text{--}8/\text{group}$. (j) Hindpaw swing speed and time on hindpaw were measured by Catwalk digital gait analysis. At PSD63, *Cre*-injected stroke mice displayed a significant impairment compared to *Cre*-injected sham controls in both parameters. *Neurod1*-treated mice were not significantly different from controls in either task. * $p < 0.05$. $n = 22\text{--}30/\text{group}$. Data are expressed as mean \pm SEM.

We predicted that perilesional reactive astrocytes would be transduced following stroke and *Neurod1* treatment. To test this, we isolated GLAST+ astrocytes from the cortex of R26R-YFP mice at 3 days post-AAV (PSD10). The number of transduced (YFP+) cells within this population was analyzed using magnetically activated cell sorting. As shown in Figure 1e, 50% of perilesional GLAST+ astrocytes expressed YFP. We next examined the ectopic expression of *Neurod1* over time in the stroke-injured brain. Using both R26R-YFP and R26R-tdTomato mice, we visualized the colocalization of neural phenotypes in fluorescent positive cells (XFP+) at early (PSD28) and late (PSD63) times post-stroke. We quantified the proportion of transduced cells that co-expressed the NeuN and GFAP markers after *Neurod1* or *Cre* was delivered. On PSD 28, following *Neurod1* injection, we observed $21.2 \pm 4.9\%$ of all XFP+ cells expressed NeuN, and $46.9 \pm 13.4\%$ expressed GFAP (Figure 1f,g). There were significantly fewer XFP+NeuN+ cells on PSD28 in the AAV5::*Cre*-injected mice ($8.3 \pm 1.7\%$, $p < 0.05$) and similar numbers of XFP+GFAP+ cells ($59.1 \pm 9.1\%$) (Figure 1f,g). Most interesting, by PSD 63, the relative percentage of NeuN+XFP+ cells in *Neurod1* injected mice was $55.0 \pm 2.4\%$, significantly greater than that of *Cre*-injected brains ($40.9 \pm 5.7\%$; $p = 0.044$; Figure 1f,h) and this was significantly increased from PSD28 ($p = 0.0009$). No change was seen in the relative percentage of XFP+GFAP+ astrocytes at PSD28 and PSD63 in any of the groups. Notably, there was a significant decrease in the relative fraction of XFP+GFAP-NeuN- cells at PSD63 in *Neurod1*-injected mice when compared to *Cre* controls (stroke/*Cre*_63d, 19.0 ± 2.7 vs. stroke/*Neurod1*_63d, 11.1 ± 1.5 ; $p = 0.022$). Hence, while the percentage of NeuN+ cells expressing *Cre* is increasing over time, the relative percentage of XFP+NeuN+ cells is significantly greater with ectopic expression of *Neurod1*.

3.2. Functional Recovery Is Observed following Ectopic Expression of *Neurod1*

We investigated the impact of ectopic *Neurod1* expression on post-stroke recovery. Stroke-injured mice that received *Neurod1* or *Cre* in the stroke-injured cortex on PSD7 were assessed for motor function using the grid walk task at PSD28 and CatWalk for gait analysis at PSD63. Stroke-injured mice displayed a significant motor deficit on the grid walking task at PSD4 prior to treatment with *Cre* or *Neurod1* ($p = 0.003$, $p = 0.002$, respectively) (Figure 1i). As predicted, uninjured mice and sham controls did not show deficits (Figure 1i). By PSD28, only mice that received *Cre* were recovered to baseline performance [stroke/*Neurod1* = 0.22 ± 0.53 slips ($p = 0.846$); stroke/*Cre* = 1.58 ± 0.26 slips ($p = 0.005$); sham/*Cre*, 1.91 ± 0.37 slips ($p = 0.0004$); uninjured controls, -0.15 ± 0.34 slips] (Figure 1i).

Since foot fault deficits are not sustained at longer survival times [49,50], and because an impairment was detected at PSD28 in sham mice that received cortical injections of *Cre* (Figure 1i), we performed gait analysis at PSD63 to compare long-term outcomes of

ectopic *Neurod1* expression [51]. Significant deficits were detected in stroke/*Cre* mice in swing speed ($5.5 \pm 1.63\%$ change; $p = 0.026$) and time spent on the hindpaw ($10.60 \pm 3.79\%$ change; $p = 0.025$) (Figure 1j). The gait of *Neurod1*-treated mice was indistinguishable from that of uninjured controls, changing $0.00 \pm 2.15\%$ in swing speed ($p = 0.67$) and $2.02 \pm 1.79\%$ in time spent on the hindpaw ($p = 0.87$) (Figure 1j). Taken together, these findings reveal that ectopic expression of *Neurod1* is sufficient to improve functional outcomes following stroke as early as 3 weeks post-transduction and maintain recovery to at least 8 weeks post-intervention.

3.3. The Percent of Transduced Neurons in the Perilesional Cortex Increases over Time

We predicted that improved functional outcomes would be correlated with increased numbers of XFP+NeuN+ cells in the perilesional cortex. We quantified the relative percent of transduced perilesional neurons (NeuN+XFP+/NeuN+) at 21 and 56 days post-AAV transduction in stroke-injured and sham-injected mice. In the stroke-injured mice, there were significantly more XFP+ neurons in *Neurod1* ($2.78 \pm 0.7\%$ and $20.2 \pm 3.1\%$, at day 21 and day 56, respectively) compared to *Cre*-injected brains ($0.47 \pm 0.26\%$ and $4.67 \pm 0.91\%$, at day 21 and day 56, respectively) ($p = 0.031$ for day 28 and $p < 0.0001$ for day 56) (Figure 2a). Further, the relative percentage of NeuN+XFP+/NeuN+ cells in the stroke-injured mice was significantly greater at PSD63 compared to PSD28 ($p = 0.030$). These findings indicate that the relative percentage of transduced neurons in the perilesional cortex is significantly greater in stroke-injured mice following the ectopic expression of *Neurod1*.

To compare the proportions of transduced neurons in the absence of injury, we delivered *Neurod1* and *Cre* to sham animals and quantified the transduced cells that co-expressed NeuN in the equivalent cortical area and time points examined above. We predicted that sham animals that received *Neurod1* would have more XFP+NeuN+ cells following treatment. As predicted, those mice that received AAV5::*Neurod1* had more XFP+NeuN+ cells compared to controls that did not receive *Neurod1* (*Neurod1*, $8.1 \pm 1.5\%$ and $11.8 \pm 1.0\%$ of total neurons at day 21 and day 56, respectively; *Cre*, $1.4 \pm 1.0\%$ and $3.9 \pm 0.3\%$ at day 21 and day 56, respectively) ($p < 0.05$) (Figure 2a).

We sought to determine the cellular phenotypes associated with the observed long-term motor recovery. We analyzed the expression of neuronal subtype-specific transcription factors CUX1 (upper-layer neurons, layers 2/3 [52]) and CTIP2 (lower-layer projection neurons, layers 5/6 [53]) at PSD63 in R26R-YFP mice that received *Neurod1* post-stroke (Figure 2b). We observed CUX1 exclusively in YFP+NeuN+ cells in the upper layers. Similarly, CTIP2 was only present in YFP+NeuN+ neurons in the lower layers. We performed immunohistochemistry for c-FOS as an indicator of neuronal activity and found that a subpopulation of the YFP+NeuN+ neurons co-expressed c-FOS within the cortex (Figure 2c). Hence, neurons expressing *Neurod1* are active within the cortex at a time when functional recovery is observed.

We next asked whether the improved outcomes following *Neurod1* treatment were associated with a change in lesion volume. We compared the brains of stroke-injured *Neurod1* and *Cre*-injected animals at PSD63 and found similar lesion volumes (stroke/*Neurod1* = $0.06 \pm 0.03 \text{ mm}^3$; stroke/*Cre* = $0.07 \pm 0.01 \text{ mm}^3$; $p = 0.62$) (Figure S1). Hence, ectopic expression of *Neurod1* does not lead to a change in lesion volume at long survival times and when functional recovery is observed.

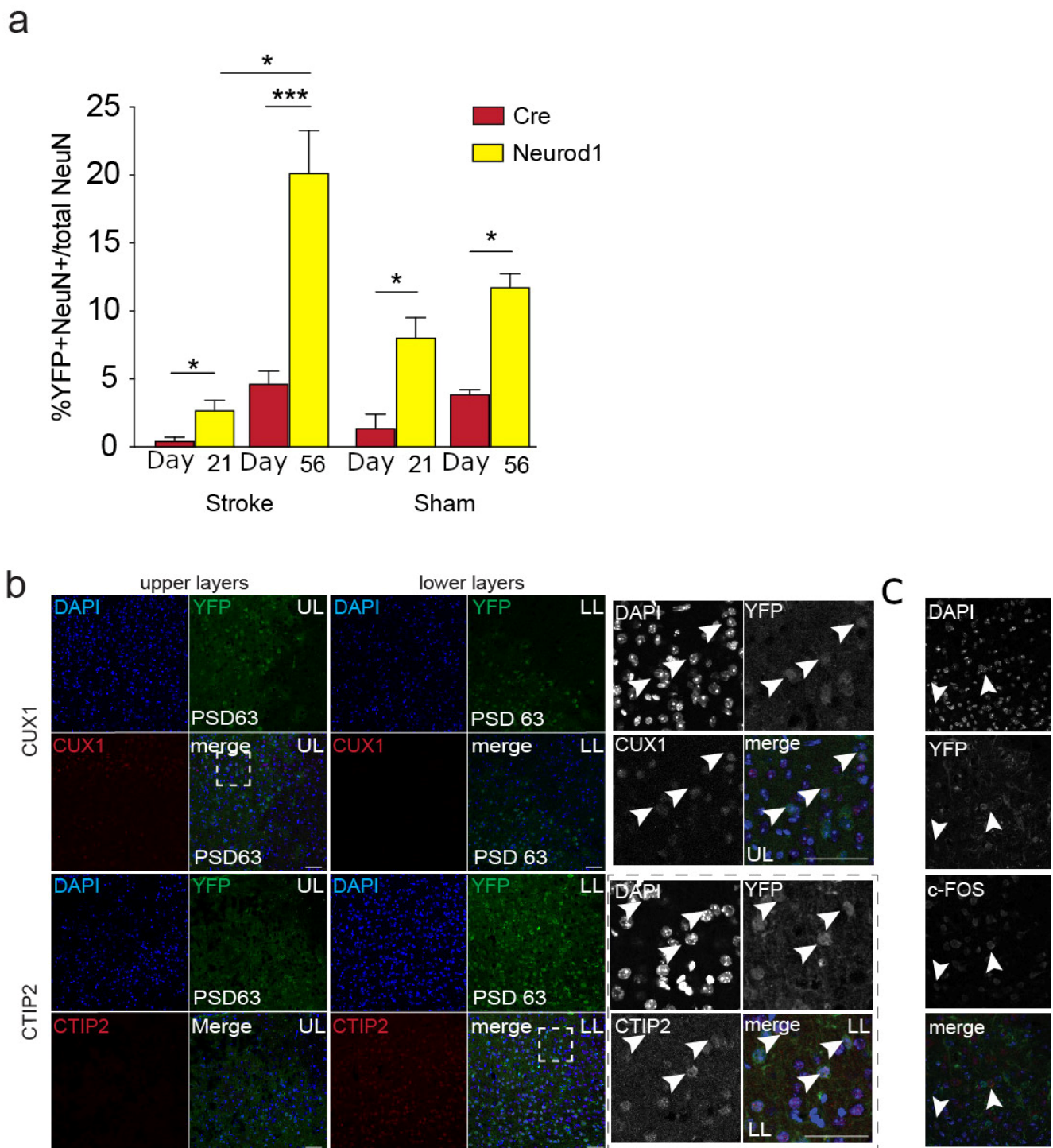


Figure 2. Characterization of cell types produced following AAV5 delivery of *Neurod1*. (a) Percentage of XFP+NeuN+ neurons of the total perilesional neurons following stroke or sham injury on day 28 and day 63. * $p < 0.05$, *** $p < 0.001$; $n = 3-16$ /group. (b) Representative images of CUX1+ and YFP+CTIP2+ neurons in the upper (UL) and lower (LL) layers. White dashed box shows position of enlarged images of CUX1+ cells in the UL and CTIP2+ cells in the LL. Arrowheads indicate examples of layer marker+YFP+ neurons. (c) Example image of c-FOS expression in NeuN+YFP+ reprogrammed neurons. Arrowheads indicate examples of c-FOS+YFP+ neurons.

4. Discussion

Here, we demonstrate that ectopic expression of *Neurod1* is sufficient for functional improvement following sensory–motor stroke. Previous studies have used AAV delivery to ectopically express TFs in vivo [11,14,15,28,32,40,41,54,55]; however, few have demonstrated improved functional outcomes following injury [41,42]. Using the grid walk task and gait analysis, we demonstrate that ectopic expression of *Neurod1* in the stroke-injured brain leads to functional improvement as early as three weeks post *Neurod1* delivery and that the recovery is sustained long-term.

Studying functional outcomes in rodent stroke models is important for determining the preclinical efficacy of interventions. However, this is difficult due to two main elements: (1) the equivalent cellular processes thought to underlie post-stroke neuroregenerative and neuroplastic processes (thought to recapitulate processes that occur in development to some degree) occur in an abbreviated time frame compared to those observed in the clinic (reviewed by [56]); and (2) spontaneous recovery of most widely validated post-stroke behavioral tests (including those used here) can occur within weeks in rodents models, as opposed to the persistent, attenuated timeframes seen in human stroke survivors. As such, the Stroke Therapy Academic Industry Roundtable Preclinical Recommendations [43] suggest that rodent stroke models include long-term outcomes measuring at least 2–3 weeks after stroke. In this study, our 9-week timeline exceeding this recommendation is considered chronic in terms of rodent stroke models [57], and importantly, it was still able to detect deficits in untreated controls that were significantly improved in *Neurod1*-treated animals. This finding has important implications for preclinical stroke research.

Chen and colleagues [42] examined the effects of ectopic expression of *Neurod1* following stroke and reported similar outcomes while highlighting some important considerations for stroke studies. First, Chen et al. [42] used a dual AAV9 system (where *Neurod1* expression is driven by a CAG promoter) following ET-1 stroke-injured mice and found that 70% of all transduced cells expressed the neuronal marker NeuN at 14 days post-stroke. We observed NeuN expression in 21% of transduced cells over a similar time course using a single AAV5 system, where the expression of *Neurod1* was driven by the GFAP promoter. Further, our studies did not reveal a difference in the lesion volume in our stroke-injured mice that received *Neurod1*, which was significantly reduced following *Neurod1* expression in the previous work. Different strains of mice, the severity and location of the injury, the time course for intervention, concentration, and serotype of the AAV are also likely to play a role in the outcomes. Importantly, we showed that a lower conversion efficiency also results in long-term recovery. A comparison of these studies is critical when developing therapeutics to treat stroke and reflects the complexity of the model and the importance of demonstrating success in more than one pre-clinical model of injury to improve the potential for translational success of novel therapeutics.

Interestingly, we found that the proportion of transduced neurons in *Neurod1*-treated mice was significantly increased compared to *Cre* controls at PSD28, a time at which functional recovery was already observed. Similarly, we show that transduced neurons comprise almost 20% of the perilesional population in *Neurod1*-treated mice and express markers of activity and regional specificity. When interpreting our findings, it is important to note that we also observed reporter-positive neurons in *Cre*-injected mice (i.e., in the absence of *Neurod1* delivery). This is interesting and consistent with previous work showing a degree of non-specific expression from the GFAP promoter [28,34,35,58]. This reveals the importance of future studies aimed at discerning whether improved recovery is mediated by the conversion of astrocytes to neurons or other mechanisms, such as enhanced neuronal cell survival and/or neuroprotection as a result of ectopic *Neurod1* expression. An eloquent study has recently demonstrated that the ablation of induced neurons generated from microglia/macrophages following a stroke that encompasses the striatum (middle cerebral artery occlusion) leads to the loss of functional improvements [59]. As we move forward in the field, a recent position paper that outlines the obligatory controls for demonstrating in vivo neuronal reprogramming will provide important guidance. Bocchi et al. [60] include

lineage tracing (neuronal and glial), single-cell transcriptomics studies, and functional assessment of induced neurons as important next steps.

Recent papers are drawing attention to the poorly understood mechanism of action when reprogramming TFs are expressed in the in situ brain [34,60,61]. We demonstrated that the number of transduced neurons increases over time, and this is correlated with improved functional outcomes. This temporal increase could be the result of astrocyte-to-neuron reprogramming, as well as delayed expression of the AAV in neurons due to leakiness of the promoter. These possibilities are consistent with the observation that at early times post-AAV delivery, the vast majority of transduced cells did not express neuronal markers, and over 50% of the cortical astrocytes in the perilesional stroke area were transduced with the AAV. Studies revealing the extent of astrocyte heterogeneity raise the possibility that functional recovery could also be due to a shift in astrocyte cell state due to ectopic expression of TFs [62,63]. Indeed, specifically blocking a subset of reactive astrocytes was shown to be neuroprotective in a model of Parkinson's disease [64], and ectopic expression of *Neurod1* in astrocytes may specifically decrease this reactive astrocyte population [65].

We chose to use AAV5 to deliver *Neurod1* based on previous work suggesting enhanced astrocyte targeting with this serotype [46]. A number of different viral delivery methods have been used for in vivo reprogramming (e.g., lentivirus, adenovirus, and AAV9 [66]). These have shown varied transduction and reprogramming efficiencies. Different delivery methods may preferentially transduce different astrocyte subtypes or other neural cell types, highlighting the importance of choosing an appropriate strategy. In our study, AAV5 was used to drive *Neurod1* expression under the control of the short GFAP (gfaABC(1)D) promoter. We performed reprogramming at 7 days post-stroke in order to preferentially target cortical astrocytes and not neural stem cells that also express GFAP [67–70], as this is a time we have previously demonstrated a rapid decline in the number of migratory neural stem cells present in the cortex by this time point [71].

With the goal of realizing the translational potential of gene therapies that deliver neurogenic TFs to treat the injured or diseased brain, a comprehensive understanding of the cellular and molecular basis of functional recovery is an important consideration for future studies exploring gene therapy-based approaches for stroke repair. Herein, we have demonstrated that the AAV5-mediated expression of *Neurod1* driven by the shGFAP promoter leads to post-stroke functional recovery. Our work highlights the promise of this strategy for stroke repair.

Supplementary Materials: The following supporting information can be downloaded at: <https://www.mdpi.com/article/10.3390/biomedicines12030663/s1>, Figure S1. Lesion volume. Volume (mm³) of the lesion was similar between stroke animals that received *Neurod1* (stroke_nd1) and *Cre* (stroke_cre) injections. $p > 0.05$. $n = 6–8$ /group. Data are expressed as mean \pm SEM.

Author Contributions: Conceptualization, C.M.M.; Methodology, J.M.L., T.T.L., T.E., C.M.P., A.K., K.W.A.B., B.W.D., O.S.I., N.S., D.L.C. and A.O.; Formal analysis, J.M.L., T.T.L., T.E., E.D., C.M.P., A.K., K.W.A.B., I.K., O.S.I., N.S. and C.M.M.; Writing—original draft, J.M.L. and C.M.M.; Writing—review & editing, J.M.L. and C.M.M.; Visualization, C.M.M.; Supervision, C.M.M.; Funding acquisition, C.M.M. All authors have read and agreed to the published version of the manuscript.

Funding: This work was supported by grants to C.M.M. from the Heart and Stroke Foundation, Ontario Institute of Regenerative Medicine, Canada First Research Excellence Fund (Medicine by Design, MbD), CIHR, and the National Sciences and Engineering Research Council (C.M.P. studentship; C.M.M.). J.M.L. held a postdoctoral fellowship (Medicine by Design, C.M.M.). The funders had no role in study design, data collection and analysis, decision to publish, or preparation of the manuscript.

Institutional Review Board Statement: The study was conducted in accordance with the Canadian Council for Animal Care, and approved by the Animal Care Committee of University of Toronto.

Informed Consent Statement: Not applicable.

Data Availability Statement: The data presented in this study are available on request from the corresponding author due to privacy.

Acknowledgments: The authors are grateful to Maryam Faiz for contributions to all aspects of the project and Ilan Vonderwalde for assistance with behavioral analyses.

Conflicts of Interest: The authors declare no conflict of interest.

References

- Virani, S.S.; Alonso, A.; Benjamin, E.J.; Bittencourt, M.S.; Callaway, C.W.; Carson, A.P.; Chamberlain, A.M.; Chang, A.R.; Cheng, S.; Delling, F.N.; et al. Heart Disease and Stroke Statistics—2020 Update: A Report from the American Heart Association. *Circulation* **2020**, *141*, E139–E596. [[CrossRef](#)] [[PubMed](#)]
- Tsao, C.W.; Aday, A.W.; Almarazooq, Z.I.; Alonso, A.; Beaton, A.Z.; Bittencourt, M.S.; Boehme, A.K.; Buxton, A.E.; Carson, A.P.; Commodore-Mensah, Y.; et al. Heart Disease and Stroke Statistics-2022 Update: A Report From the American Heart Association. *Circulation* **2022**, *145*, E153–E639. [[CrossRef](#)] [[PubMed](#)]
- Burvill, P.; Johnson, G.; Jamrozik, K.; Anderson, C.; Stewart-Wynn, E. Risk Factors for Post-Stroke Depression. *Int. J. Geriatr. Psychiatry* **1997**, *12*, 219–226. [[CrossRef](#)]
- Krueger, H.; Koot, J.; Hall, R.; O’Callaghan, C.; Bayley, M.; Corbett, D. Prevalence of Individuals Experiencing the Effects of Stroke in Canada: Trends and Projections. *Stroke* **2015**, *46*, 2226–2231. [[CrossRef](#)] [[PubMed](#)]
- Venna, V.R.; Li, J.; Hammond, M.D.; Mancini, N.S.; McCullough, L.D. Chronic Metformin Treatment Improves Post-Stroke Angiogenesis and Recovery after Experimental Stroke. *Eur. J. Neurosci.* **2014**, *39*, 2129–2138. [[CrossRef](#)]
- Dadwal, P.; Mahmud, N.; Sinai, L.; Azimi, A.; Fatt, M.; Wondisford, F.E.; Miller, F.D.; Morshead, C.M. Activating Endogenous Neural Precursor Cells Using Metformin Leads to Neural Repair and Functional Recovery in a Model of Childhood Brain Injury. *Stem Cell Rep.* **2015**, *5*, 166–173. [[CrossRef](#)] [[PubMed](#)]
- Nusrat, L.; Livingston-Thomas, J.M.; Raguthavan, V.; Adams, K.; Vonderwalde, I.; Corbett, D.; Morshead, C.M. Cyclosporin A-Mediated Activation of Endogenous Neural Precursor Cells Promotes Cognitive Recovery in a Mouse Model of Stroke. *Front. Aging Neurosci.* **2018**, *10*, 93. [[CrossRef](#)] [[PubMed](#)]
- Boese, A.C.; Le, Q.-S.E.; Pham, D.; Hamblin, M.H.; Lee, J.-P. Neural Stem Cell Therapy for Subacute and Chronic Ischemic Stroke. *Stem Cell Res. Ther.* **2018**, *9*, 154. [[CrossRef](#)]
- Vonderwalde, I.; Azimi, A.; Rolvink, G.; Ahlfors, J.; Shoichet, M.; Morshead, C. Transplantation of Directly Reprogrammed Human Neural Precursor Cells Following Stroke Promotes Synaptogenesis and Functional Recovery. *Transl. Stroke Res.* **2020**, *11*, 93–107. [[CrossRef](#)]
- Takahashi, K.; Yamanaka, S. Induction of Pluripotent Stem Cells from Mouse Embryonic and Adult Fibroblast Cultures by Defined Factors. *Cell* **2006**, *126*, 663–676. [[CrossRef](#)]
- Li, H.; Chen, G. In Vivo Reprogramming for CNS Repair: Regenerating Neurons from Endogenous Glial Cells. *Neuron* **2016**, *91*, 728–738. [[CrossRef](#)]
- Bajohr, J.; Faiz, M. Direct Lineage Reprogramming in the CNS. *Adv. Exp. Med. Biol.* **2020**, *1212*, 31–48. [[CrossRef](#)]
- Graf, T.; Enver, T. Forcing Cells to Change Lineages. *Nature* **2009**, *462*, 587–594. [[CrossRef](#)]
- Heinrich, C.; Blum, R.; Gascón, S.; Masserdotti, G.; Tripathi, P.; Sánchez, R.; Tiedt, S.; Schroeder, T.; Götz, M.; Berninger, B. Directing Astroglia from the Cerebral Cortex into Subtype Specific Functional Neurons. *PLoS Biol.* **2010**, *8*, e1000373. [[CrossRef](#)]
- Karow, M.; Sánchez, R.; Schichor, C.; Masserdotti, G.; Ortega, F.; Heinrich, C.; Gascón, S.; Khan, M.; Lie, D.; Dellavalle, A.; et al. Reprogramming of Pericyte-Derived Cells of the Adult Human Brain into Induced Neuronal Cells. *Cell Stem Cell* **2012**, *11*, 471–476. [[CrossRef](#)] [[PubMed](#)]
- Xu, J.; Du, Y.; Deng, H. Direct Lineage Reprogramming: Strategies, Mechanisms, and Applications. *Cell Stem Cell* **2015**, *16*, 119–134. [[CrossRef](#)] [[PubMed](#)]
- Masserdotti, G.; Gascón, S.; Götz, M. Direct Neuronal Reprogramming: Learning from and for Development. *Development* **2016**, *143*, 2494–2510. [[CrossRef](#)] [[PubMed](#)]
- Gascón, S.; Masserdotti, G.; Russo, G.; Götz, M. Direct Neuronal Reprogramming: Achievements, Hurdles, and New Roads to Success. *Cell Stem Cell* **2017**, *21*, 18–34. [[CrossRef](#)] [[PubMed](#)]
- Matsuda, T.; Nakashima, K. Clarifying the Ability of NeuroD1 to Convert Mouse Microglia into Neurons. *Neuron* **2021**, *109*, 3912–3913. [[CrossRef](#)] [[PubMed](#)]
- Ghazale, H.; Park, E.J.; Vasan, L.; Mester, J.; Saleh, F.; Trevisiol, A.; Zinyk, D.; Chinchalongporn, V.; Liu, M.; Fleming, T.; et al. Ascl1 Phospho-Site Mutations Enhance Neuronal Conversion of Adult Cortical Astrocytes In Vivo. *Front. Neurosci.* **2022**, *16*, 917071. [[CrossRef](#)] [[PubMed](#)]
- Zhang, Y.; Li, B.; Cananzi, S.; Han, C.; Wang, L.L.; Zou, Y.; Fu, Y.X.; Hon, G.C.; Zhang, C.L. A Single Factor Elicits Multilineage Reprogramming of Astrocytes in the Adult Mouse Striatum. *Proc. Natl. Acad. Sci. USA* **2022**, *119*, e2107339119. [[CrossRef](#)] [[PubMed](#)]
- Talifu, Z.; Liu, J.Y.; Pan, Y.Z.; Ke, H.; Zhang, C.J.; Xu, X.; Gao, F.; Yu, Y.; Du, L.J.; Li, J.J. In Vivo Astrocyte-to-Neuron Reprogramming for Central Nervous System Regeneration: A Narrative Review. *Neural Regen. Res.* **2023**, *18*, 750–755. [[CrossRef](#)]

23. Grande, A.; Sumiyoshi, K.; López-Juárez, A.; Howard, J.; Sakthivel, B.; Aronow, B.; Campbell, K.; Nakafuku, M. Environmental Impact on Direct Neuronal Reprogramming In Vivo in the Adult Brain. *Nat. Commun.* **2013**, *4*, 2373. [[CrossRef](#)]
24. Chanda, S.; Ang, C.E.; Davila, J.; Pak, C.; Mall, M.; Lee, Q.Y.; Ahlenius, H.; Jung, S.W.; Südhof, T.C.; Wernig, M. Generation of Induced Neuronal Cells by the Single Reprogramming Factor ASCL1. *Stem Cell Rep.* **2014**, *3*, 282–296. [[CrossRef](#)]
25. Puls, B.; Ding, Y.; Zhang, F.; Pan, M.; Lei, Z.; Pei, Z.; Jiang, M.; Bai, Y.; Forsyth, C.; Metzger, M.; et al. Regeneration of Functional Neurons After Spinal Cord Injury via in Situ NeuroD1-Mediated Astrocyte-to-Neuron Conversion. *Front. Cell Dev. Biol.* **2020**, *8*, 591883. [[CrossRef](#)] [[PubMed](#)]
26. Ge, L.J.; Yang, F.H.; Li, W.; Wang, T.; Lin, Y.; Feng, J.; Chen, N.H.; Jiang, M.; Wang, J.H.; Hu, X.T.; et al. In Vivo Neuroregeneration to Treat Ischemic Stroke Through NeuroD1 AAV-Based Gene Therapy in Adult Non-Human Primates. *Front. Cell Dev. Biol.* **2020**, *8*, 590008. [[CrossRef](#)]
27. Vasan, L.; Park, E.; David, L.A.; Fleming, T.; Schuurmans, C. Direct Neuronal Reprogramming: Bridging the Gap Between Basic Science and Clinical Application. *Front. Cell Dev. Biol.* **2021**, *9*, 681087. [[CrossRef](#)]
28. Mattugini, N.; Bocchi, R.; Scheuss, V.; Russo, G.L.; Torper, O.; Lao, C.L.; Götz, M. Inducing Different Neuronal Subtypes from Astrocytes in the Injured Mouse Cerebral Cortex. *Neuron* **2019**, *103*, 1086–1095.e5. [[CrossRef](#)]
29. Herrero-Navarro, Á.; Puche-Aroca, L.; Moreno-Juan, V.; Sempere-Ferrández, A.; Espinosa, A.; Susín, R.; Torres-Masjoan, L.; Leyva-Díaz, E.; Karow, M.; Figueres-Oñate, M.; et al. Astrocytes and Neurons Share Region-Specific Transcriptional Signatures That Confer Regional Identity to Neuronal Reprogramming. *Sci. Adv.* **2021**, *7*, eabe8978. [[CrossRef](#)]
30. Pfisterer, U.; Kirkeby, A.; Torper, O.; Wood, J.; Nelander, J.; Dufour, A.; Björklund, A.; Lindvall, O.; Jakobsson, J.; Parmar, M. Direct Conversion of Human Fibroblasts to Dopaminergic Neurons. *Proc. Natl. Acad. Sci. USA* **2011**, *108*, 10343–10348. [[CrossRef](#)]
31. Heinrich, C.; Götz, M.; Berninger, B. Reprogramming of Postnatal Astroglia of the Mouse Neocortex into Functional, Synapse-Forming Neurons. *Methods Mol. Biol.* **2012**, *814*, 485–498. [[CrossRef](#)] [[PubMed](#)]
32. Liu, Y.; Miao, Q.; Yuan, J.; Han, S.; Zhang, P.; Li, S.; Rao, Z.; Zhao, W.; Ye, Q.; Geng, J.; et al. Ascl1 Converts Dorsal Midbrain Astrocytes into Functional Neurons In Vivo. *J. Neurosci.* **2015**, *35*, 9336–9355. [[CrossRef](#)]
33. Vadodaria, K.; Mertens, J.; Paquola, A.; Bardy, C.; Li, X.; Jappelli, R.; Fung, L.; Marchetto, M.; Hamm, M.; Gorris, M.; et al. Generation of Functional Human Serotonergic Neurons from Fibroblasts. *Mol. Psychiatry* **2016**, *21*, 49–61. [[CrossRef](#)] [[PubMed](#)]
34. Wang, L.L.; Serrano, C.; Zhong, X.; Ma, S.; Zou, Y.; Zhang, C.L. Revisiting Astrocyte to Neuron Conversion with Lineage Tracing In Vivo. *Cell* **2021**, *184*, 5465–5481.e16. [[CrossRef](#)] [[PubMed](#)]
35. Xie, Y.; Zhou, J.; Wang, L.L.; Zhang, C.L.; Chen, B. New AAV Tools Fail to Detect NeuroD1-Mediated Neuronal Conversion of Müller Glia and Astrocytes In Vivo. *EBioMedicine* **2023**, *90*, 1–19. [[CrossRef](#)]
36. Xiang, Z.; Xu, L.; Liu, M.; Wang, Q.; Li, W.; Lei, W.; Chen, G. Lineage Tracing of Direct Astrocyte-to-Neuron Conversion in the Mouse Cortex. *Neural Regen. Res.* **2021**, *16*, 750–756. [[CrossRef](#)]
37. Götz, M.; Bocchi, R. Neuronal Replacement: Concepts, Achievements, and Call for Caution. *Curr. Opin. Neurobiol.* **2021**, *69*, 185–192. [[CrossRef](#)]
38. Barker, R.A.; Götz, M.; Parmar, M. New Approaches for Brain Repair—from Rescue to Reprogramming. *Nature* **2018**, *557*, 329–334. [[CrossRef](#)]
39. Sharif, N.; Calzolari, F.; Berninger, B. Direct In Vitro Reprogramming of Astrocytes into Induced Neurons. *Methods Mol. Biol.* **2021**, *2352*, 13–29. [[CrossRef](#)]
40. Guo, Z.; Zhang, L.; Wu, Z.; Chen, Y.; Wang, F.; Chen, G. In Vivo Direct Reprogramming of Reactive Glial Cells into Functional Neurons after Brain Injury and in an Alzheimer’s Disease Model. *Cell Stem Cell* **2014**, *14*, 188–202. [[CrossRef](#)]
41. Rivetti di Val Cervo, P.; Romanov, R.; Spigolon, G.; Masini, D.; Martín-Montañez, E.; Toledo, E.; La Manno, G.; Feyder, M.; Pifl, C.; Ng, Y.; et al. Induction of Functional Dopamine Neurons from Human Astrocytes In Vitro and Mouse Astrocytes in a Parkinson’s Disease Model. *Nat. Biotechnol.* **2017**, *35*, 444–452. [[CrossRef](#)]
42. Chen, Y.C.; Ma, N.X.; Pei, Z.F.; Wu, Z.; Do-Monte, F.H.; Keefe, S.; Yellin, E.; Chen, M.S.; Yin, J.C.; Lee, G.; et al. A NeuroD1 AAV-Based Gene Therapy for Functional Brain Repair after Ischemic Injury through In Vivo Astrocyte-to-Neuron Conversion. *Mol. Ther.* **2020**, *28*, 217–234. [[CrossRef](#)] [[PubMed](#)]
43. Lapchak, P.A.; Zhang, J.H.; Noble-Haeusslein, L.J. RIGOR Guidelines: Escalating STAIR and STEPS for Effective Translational Research. *Transl. Stroke Res.* **2013**, *4*, 279–285. [[CrossRef](#)] [[PubMed](#)]
44. Roome, R.B.; Bartlett, R.F.; Jeffers, M.; Xiong, J.; Corbett, D.; Vanderluit, J.L. A Reproducible Endothelin-1 Model of Forelimb Motor Cortex Stroke in the Mouse. *J. Neurosci. Methods* **2014**, *233*, 34–44. [[CrossRef](#)] [[PubMed](#)]
45. Horie, N.; Maag, A.-L.; Hamilton, S.A.; Shichinohe, H.; Bliss, T.M.; Steinberg, G.K. Mouse Model of Focal Cerebral Ischemia Using Endothelin-1. *J. Neurosci. Methods* **2008**, *173*, 286–290. [[CrossRef](#)] [[PubMed](#)]
46. Merienne, N.; Le Douce, J.; Faivre, E.; Déglon, N.; Bonvento, G. Efficient Gene Delivery and Selective Transduction of Astrocytes in the Mammalian Brain Using Viral Vectors. *Front. Cell Neurosci.* **2013**, *7*, 54254. [[CrossRef](#)]
47. Srinivas, S.; Watanabe, T.; Lin, C.S.; William, C.M.; Tanabe, Y.; Jessell, T.M.; Costantini, F. Cre Reporter Strains Produced by Targeted Insertion of EYFP and ECFP into the ROSA26 Locus. *BMC Dev. Biol.* **2001**, *1*, 4. [[CrossRef](#)]
48. Tennant, K.A.; Jones, T.A. Sensorimotor Behavioral Effects of Endothelin-1 Induced Small Cortical Infarcts in C57BL/6 Mice. *J. Neurosci. Methods* **2009**, *181*, 18–26. [[CrossRef](#)]
49. Murphy, T.; Corbett, D. Plasticity during Stroke Recovery: From Synapse to Behaviour. *Nat. Rev. Neurosci.* **2009**, *10*, 861–872. [[CrossRef](#)]

50. Ito, M.; Aswendt, M.; Lee, A.; Ishizaka, S.; Cao, Z.; Wang, E.; Levy, S.; Smerin, D.; McNab, J.; Zeineh, M.; et al. RNA-Sequencing Analysis Revealed a Distinct Motor Cortex Transcriptome in Spontaneously Recovered Mice After Stroke. *Stroke* **2018**, *49*, 2191–2199. [[CrossRef](#)] [[PubMed](#)]
51. Neumann, M.; Wang, Y.; Kim, S.; Hong, S.; Jeng, L.; Bilgen, M.; Liu, J. Assessing Gait Impairment Following Experimental Traumatic Brain Injury in Mice. *J. Neurosci. Methods* **2009**, *176*, 34–44. [[CrossRef](#)] [[PubMed](#)]
52. Cubelos, B.; Briz, C.G.; Esteban-Ortega, G.M.; Nieto, M. Cux1 and Cux2 Selectively Target Basal and Apical Dendritic Compartments of Layer II-III Cortical Neurons. *Dev. Neurobiol.* **2015**, *75*, 163–172. [[CrossRef](#)] [[PubMed](#)]
53. Arlotta, P.; Molyneaux, B.J.; Jabaudon, D.; Yoshida, Y.; Macklis, J.D. Ctip2 Controls the Differentiation of Medium Spiny Neurons and the Establishment of the Cellular Architecture of the Striatum. *J. Neurosci.* **2008**, *28*, 622–632. [[CrossRef](#)] [[PubMed](#)]
54. Torper, O.; Pfisterer, U.; Wolf, D.A.; Pereira, M.; Lau, S.; Jakobsson, J.; Björklund, A.; Grealish, S.; Parmar, M. Generation of Induced Neurons via Direct Conversion In Vivo. *Proc. Natl. Acad. Sci. USA* **2013**, *110*, 7038–7043. [[CrossRef](#)] [[PubMed](#)]
55. Tao, Y.; Ma, L.; Liao, Z.; Le, Q.; Yu, J.; Liu, X.; Li, H.; Chen, Y.; Zheng, P.; Yang, Z.; et al. Astroglial β -Arrestin1-Mediated Nuclear Signaling Regulates the Expansion of Neural Precursor Cells in Adult Hippocampus. *Sci. Rep.* **2015**, *5*, 15506. [[CrossRef](#)] [[PubMed](#)]
56. Dromerick, A.W.; Edwardson, M.A.; Edwards, D.F.; Giannetti, M.L.; Barth, J.; Brady, K.P.; Chan, E.; Tan, M.T.; Tamboli, I.; Chia, R.; et al. Critical Periods after Stroke Study: Translating Animal Stroke Recovery Experiments into a Clinical Trial. *Front. Hum. Neurosci.* **2015**, *9*, 136450. [[CrossRef](#)]
57. De Boer, A.; Storm, A.; Gomez-Soler, M.; Smolders, S.; Rué, L.; Poppe, L.; B Pasquale, E.; Robberecht, W.; Lemmens, R. Environmental Enrichment during the Chronic Phase after Experimental Stroke Promotes Functional Recovery without Synergistic Effects of EphA4 Targeted Therapy. *Hum. Mol. Genet.* **2020**, *29*, 605–617. [[CrossRef](#)]
58. Lee, Y.; Messing, A.; Su, M.; Brenner, M. GFAP Promoter Elements Required for Region-Specific and Astrocyte-Specific Expression. *Glia* **2008**, *56*, 481–493. [[CrossRef](#)]
59. Irie, T.; Matsuda, T.; Hayashi, Y.; Matsuda-Ito, K.; Kamiya, A.; Masuda, T.; Prinz, M.; Isobe, N.; Kira, J.I.; Nakashima, K. Direct Neuronal Conversion of Microglia/Macrophages Reinstates Neurological Function after Stroke. *Proc. Natl. Acad. Sci. USA* **2023**, *120*, e2307972120. [[CrossRef](#)]
60. Bocchi, R.; Masserdotti, G.; Götz, M. Direct Neuronal Reprogramming: Fast Forward from New Concepts toward Therapeutic Approaches. *Neuron* **2022**, *110*, 366–393. [[CrossRef](#)]
61. Rao, Y.; Du, S.; Yang, B.; Wang, Y.; Li, Y.; Li, R.; Zhou, T.; Du, X.; He, Y.; Wang, Y.; et al. NeuroD1 Induces Microglial Apoptosis and Cannot Induce Microglia-to-Neuron Cross-Lineage Reprogramming. *Neuron* **2021**, *109*, 4094–4108.e5. [[CrossRef](#)] [[PubMed](#)]
62. Zamanian, J.; Xu, L.; Foo, L.; Nouri, N.; Zhou, L.; Giffard, R.; Barres, B. Genomic Analysis of Reactive Astroglia. *J. Neurosci.* **2012**, *32*, 6391–6410. [[CrossRef](#)]
63. Liddel, S.; Guttenplan, K.; Clarke, L.; Bennett, F.; Bohlen, C.; Schirmer, L.; Bennett, M.; Münch, A.; Chung, W.; Peterson, T.; et al. Neurotoxic Reactive Astrocytes Are Induced by Activated Microglia. *Nature* **2017**, *541*, 481–487. [[CrossRef](#)] [[PubMed](#)]
64. Yun, S.; Kam, T.; Panicker, N.; Kim, S.; Oh, Y.; Park, J.; Kwon, S.; Park, Y.; Karuppagounder, S.; Park, H.; et al. Block of A1 Astrocyte Conversion by Microglia Is Neuroprotective in Models of Parkinson’s Disease. *Nat. Med.* **2018**, *24*, 931–938. [[CrossRef](#)] [[PubMed](#)]
65. Zhang, L.; Lei, Z.; Guo, Z.; Pei, Z.; Chen, Y.; Zhang, F.; Cai, A.; Mok, G.; Lee, G.; Swaminathan, V.; et al. Development of Neuroregenerative Gene Therapy to Reverse Glial Scar Tissue Back to Neuron-Enriched Tissue. *Front. Cell Neurosci.* **2020**, 1–19. [[CrossRef](#)]
66. Chen, G.; Wernig, M.; Berninger, B.; Nakafuku, M.; Parmar, M.; Zhang, C.L. In Vivo Reprogramming for Brain and Spinal Cord Repair. *eNeuro* **2015**, *2*. [[CrossRef](#)]
67. Lois, C.; Alvarez-Buylla, A. Long-Distance Neuronal Migration in the Adult Mammalian Brain. *Science* **1994**, *264*, 1145–1148. [[CrossRef](#)]
68. Doetsch, F.; García-Verdugo, J.M.; Alvarez-Buylla, A. Regeneration of a Germinal Layer in the Adult Mammalian Brain. *Proc. Natl. Acad. Sci. USA* **1999**, *96*, 11619–11624. [[CrossRef](#)]
69. Imura, T.; Kornblum, H.; Sofroniew, M. The Predominant Neural Stem Cell Isolated from Postnatal and Adult Forebrain but Not Early Embryonic Forebrain Expresses GFAP. *J. Neurosci.* **2003**, *23*, 2824–2832. [[CrossRef](#)]
70. Morshead, C.; Garcia, A.; Sofroniew, M.; van Der Kooy, D. The Ablation of Glial Fibrillary Acidic Protein-Positive Cells from the Adult Central Nervous System Results in the Loss of Forebrain Neural Stem Cells but Not Retinal Stem Cells. *Eur. J. Neurosci.* **2003**, *18*, 76–84. [[CrossRef](#)]
71. Faiz, M.; Sachewsky, N.; Gascón, S.; Bang, K.; Morshead, C.; Nagy, A. Adult Neural Stem Cells from the Subventricular Zone Give Rise to Reactive Astrocytes in the Cortex after Stroke. *Cell Stem Cell* **2015**, *17*, 624–634. [[CrossRef](#)] [[PubMed](#)]

Disclaimer/Publisher’s Note: The statements, opinions and data contained in all publications are solely those of the individual author(s) and contributor(s) and not of MDPI and/or the editor(s). MDPI and/or the editor(s) disclaim responsibility for any injury to people or property resulting from any ideas, methods, instructions or products referred to in the content.